

Structural Analysis of a Carbon Fiber Composite Propeller

Murat Işık^{1*}

¹Department of Automotive Engineering, Bursa Uludağ University, Türkiye
<https://orcid.org/0000-0002-6116-1882>

*(muratisik@uludag.edu.tr) Email of the corresponding author

(Received: 12 February 2025, Accepted: 17 February 2025)

(2nd International Conference on Recent and Innovative Results in Engineering and Technology ICRIRET, February 11-12, 2025)

ATIF/REFERENCE: Işık, M. (2025). Structural Analysis of a Carbon Fiber Composite Propeller. *International Journal of Advanced Natural Sciences and Engineering Researches*, 9(2), 276-282.

Abstract – This study explores the topology optimization of a propeller component using the finite element method in ANSYS, with the objective of minimizing material usage while maintaining structural integrity. Carbon fiber, modeled as an orthotropic material, was selected due to its superior mechanical properties, including a Young's modulus of 230 GPa in the primary loading direction. A structured optimization approach was employed. The optimization process, constrained to 500 iterations, resulted in a mass reduction of 11.86%, decreasing from 0.016404 kg to 0.014459 kg, and a volume reduction from 9113.2 mm³ to 8032.6 mm³, retaining 88.143% of the original volume. Structural analysis revealed that most regions experienced von Mises stress values below 20 GPa, with maximum stress levels exceeding 43 GPa, particularly near fixation points, contrary to expected stress distributions. These findings align with literature data emphasizing the critical role of material selection and microstructural characteristics in determining composite performance. The results validate the effectiveness of topology optimization in reducing component weight while preserving mechanical performance. This study highlights the potential application of carbon fiber reinforced composites in weight sensitive engineering fields, such as aerospace and automotive industries, where the balance between weight reduction and load bearing capacity is critical. Future work may focus on refining stress distribution patterns and further enhancing the optimization algorithm to achieve even greater material efficiency.

Keywords – Carbon Fiber Materials, FEA Analysis, Aerospace Components, Structural Analysis, Mechanical Properties.

I. INTRODUCTION

With advancing technology, engineering methods for improving designs before prototyping and manufacturing have also evolved. One of the most powerful and widely used approaches is the finite element method (FEM), which simplifies complex problems by dividing them into smaller, manageable subproblems. By discretizing geometries, approximating functions with algebraic polynomials, and solving equations at nodal points, FEM enables accurate and efficient structural analysis. This method plays a crucial role in topology optimization, where material distribution within a given design space is optimized for maximum performance. By integrating FEM with optimization algorithms, engineers can develop lightweight, high-performance structures tailored for specific applications.

Composite materials offer significant advantages over steel in automotive manufacturing, producing lighter, safer, and more fuel-efficient vehicles. A composite consists of high-performance fibers (such as carbon or glass) embedded in a matrix material (such as epoxy polymer), enhancing properties compared to individual components. Carbon fiber composites weigh about one-fifth of steel but offer comparable or superior strength, durability, and corrosion resistance [1–3]. For example, composites has been considered to have potential for reducing vehicle weight by up to 60%, significantly improving fuel efficiency [4,5]. The high strength-to-weight and stiffness-to-weight ratios of composites make them ideal for lightweight applications, such as in aerospace. Multi-layer composite laminates, in contrast to single-layer steel, can absorb more energy during a collision [6]. However, their use in the automotive industry is limited due to high material and manufacturing costs. Although carbon-based composites have been utilized for years in specialized naval vessels like submarines, they have only recently started to be adopted as propeller materials in the commercial craft and yacht industries [7]. In the present study, a structural analysis was conducted, and topology optimization was applied to the CFRP propeller material.

II. MATERIALS AND METHOD

A. A propeller geometry was selected, as is shown in Fig. 1, to apply structural analysis and achieve topology optimization using finite element method. ANSYS software was used to apply structural analysis to the selected geometry. The material selected for the topology optimization study was Carbon Fiber, with a Young's Modulus of 230 GPa, modeled as an orthotropic material in ANSYS. The material's density was set at 1800 kg/m^3 ($1.8 \times 10^{-6} \text{ kg/mm}^3$). In terms of its elastic properties, the Young's Modulus values were assigned as 230 GPa ($2.3 \times 10^{11} \text{ Pa}$) in the X-direction, and 23 GPa ($2.3 \times 10^{10} \text{ Pa}$) in both the Y- and Z-directions. The Poisson's ratios were defined as 0.2 for the XY and XZ planes, and 0.4 for the YZ plane. The shear moduli were specified as 9 GPa ($9 \times 10^9 \text{ Pa}$) in the XY and XZ planes, and 8.214 GPa ($8.214 \times 10^9 \text{ Pa}$) in the YZ plane. Nonlinear behavior was not considered in this study, as it was set to false within the simulation.

The optimization was conducted under specific settings designed to achieve efficient material distribution. The error limits were set to aggressive mechanical tolerance to assure a strong solution, while the smoothing option was set to a medium level to balance detail and computational efficiency. A smooth transition between material and void regions was ensured by selecting the inflation option for smooth transitions. The transition ratio was defined as 0.272, and the inflation element type was set to wedges to improve mesh accuracy. The optimization process was limited to a maximum of 500 iterations to ensure computational efficiency. The minimum normalized density was set to 1.0×10^{-3} , and the minimum density threshold was defined as 1.0×10^{-3} . Convergence accuracy was maintained at 0.1% to ensure the solution's precision, while a stiffness penalty factor of 3 was applied to prevent unrealistic material distribution.

The simulation was carried out following a structured procedure in ANSYS. First, a baseline solid model was created to serve as the reference geometry. Carbon Fiber was assigned as the material, with orthotropic properties specified for the simulation. A high quality mesh was generated, utilizing wedge shaped inflation elements to enhance accuracy. Appropriate boundary conditions, including constraints and loads (20 kN), were applied to simulate experimental conditions (Fig 2b). The topology optimization was then performed over 500 iterations, resulting in a final design. Post processing was conducted to analyze the mass and volume reductions, which were subsequently validated against the original design.

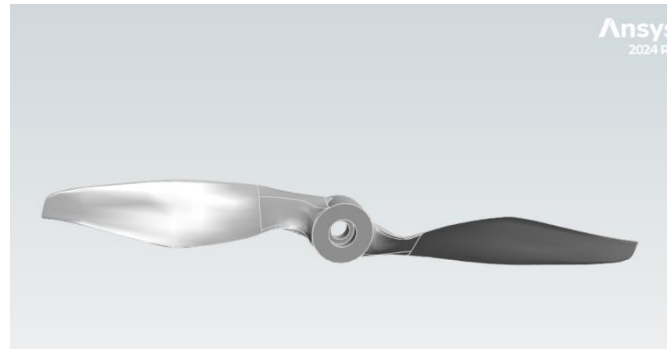


Figure. 1 CAD model of the component.

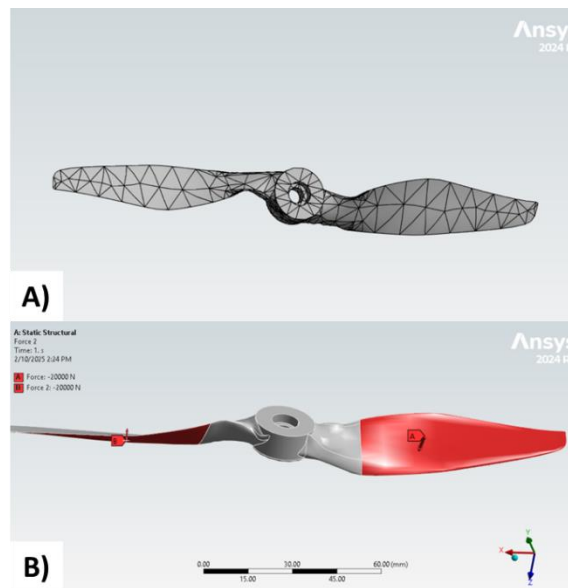


Figure. 2 Mesh structure and boundary conditions of the component.

III. RESULTS

Structural analysis was performed, and a distribution map was obtained, as shown in Figure 3. In most regions of the component, the equivalent von Mises stress values were observed to be below 20 GPa. However, the maximum stress reached approximately or exceeded 43 GPa, with the regions exhibiting these high stress values colored in red. Notably, the areas of maximum stress are located near the fixation points, contrary to the expected behavior, where the highest stresses would typically occur further away from these fixed regions. Additionally, the edges of the propeller, particularly at the tips, exhibited minimal stress levels, with values below 5 GPa. It has been observed that the different angles in A, B, and C do not show a significant difference regarding equivalent stress values.

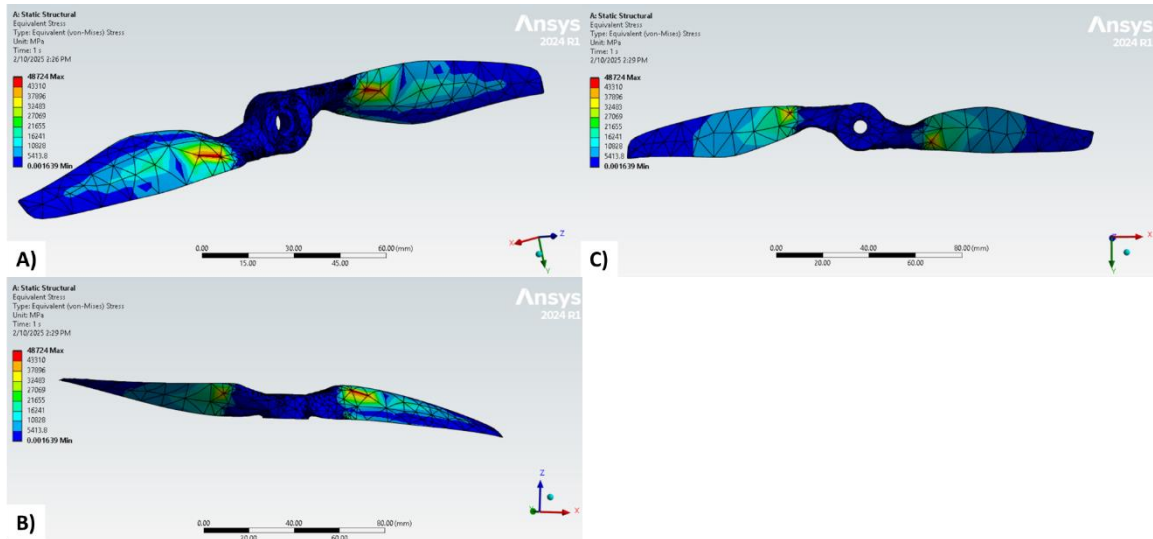


Figure. 3 Equivalent stress distribution map of the component based on structural analysis at different angles (A, B, and C).

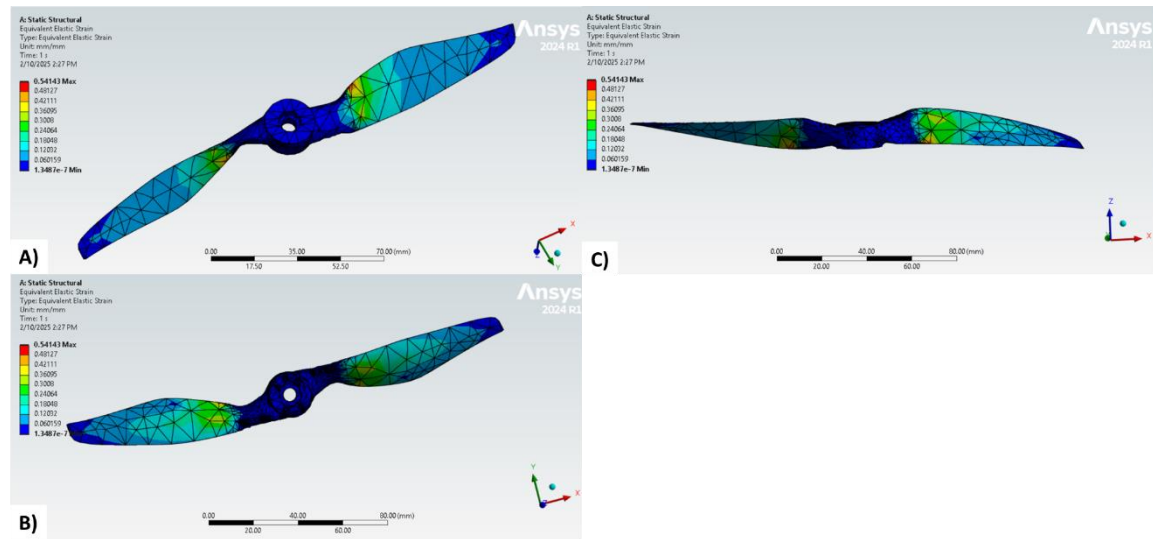


Figure. 4 Elastic strain distribution of the component obtained from structural analysis at angles A, B, and C.

The values of elastic strain exhibit different tendencies at angles A, B, and C. The maximum elastic strain values, highlighted in red, correspond to a relatively small area, around 0.54 mm/mm, in almost all the different angle views. In Fig. 4a, the majority of the distribution area shows values around 0.12 mm/mm, whereas in Fig. 4b, values close to 0.3 mm/mm are more prominent. In Fig. 4c, nearly half of the blade tip distribution find a place within the range of 0.24–0.3 mm/mm elastic strain.

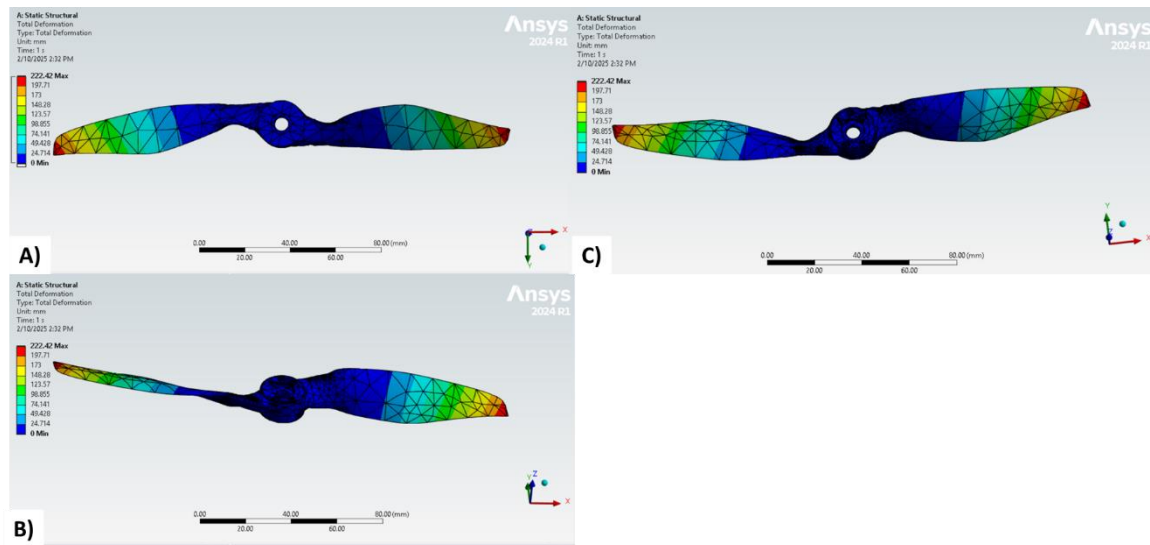


Figure 5. Distribution of total deformation in the component derived from structural analysis at angles A, B, and C

Figure 5 shows total distribution maps of the component. The maximum deformation value is approximately 222 mm at the blade tip, gradually decreasing to below 24 mm as the distance approaches the propeller fixation area. The total deformation distribution map features nearly eight color zones. The values decrease in the following order: from above 197 mm to a range between 197–173 mm, then to below 173 mm, followed by a range of 148–123 mm. The values then decrease to the 123–98 mm zone, then to the 98–74 mm zone, followed by the 74–49 mm zone. Finally, the values reach the 49–24 mm zone, and ultimately approach 0.

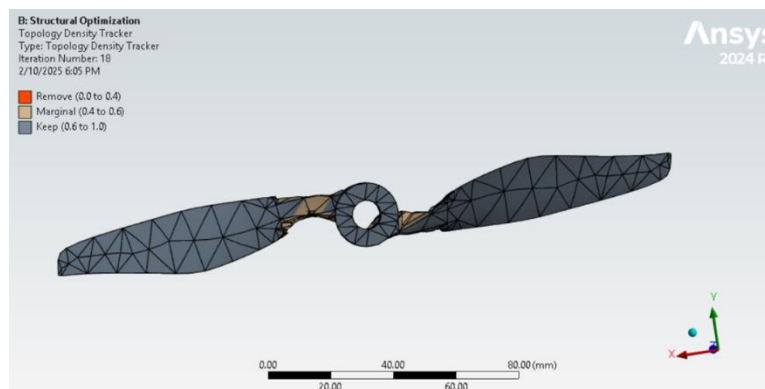


Figure 6. Topologically optimized carbon fiber propeller.

The material properties provided the necessary foundation for the subsequent topology optimization analysis. The topology optimization was performed to reduce material use while maintaining the structural integrity of the component (Fig. 6). Initially, the volume of the component was 9113.2 mm³, and after optimization, the final volume was reduced to 8032.6 mm³, which corresponds to 88.143% of the original volume being retained. The original mass of the component was 0.016404 kg, and following optimization, the mass decreased to 0.014459 kg, reflecting a reduction in material consumption while ensuring the component’s functionality. The optimized geometry achieved an 11.86% reduction in mass, demonstrating the effectiveness of the optimization process in reducing material usage while maintaining the component's required mechanical properties.

IV. DISCUSSION

The use of carbon fibers has increased significantly due to their exceptional mechanical properties. Carbon fiber reinforced thermoplastic composites have enhanced the mechanical properties of the composites. Over the past decade, the adoption of carbon fiber reinforced polymers has rapidly grown in the automotive, aerospace, and various different production industries, driven by these beneficial characteristics [8]. The superior mechanical properties of carbon fibers are closely linked to their microstructural characteristics. For instance, weak interfacial bonding between the fibers and polymer matrix can lead to poor mechanical performance in composites [9,10]. This highlights the importance of strong interfacial adhesion between fibers and polymers for achieving desirable mechanical properties. Additionally, factors such as carbon fiber concentration, the type of additives (e.g., graphene oxide or CNT) [11,12], and fiber length are also known to significantly influence mechanical performance [13]. The literature substantiates that commercial carbon fibers exhibit high tensile strength, typically ranging from 3 to 7 GPa, as well as a high Young's modulus, ranging from 200 to 500 GPa [14]. These values align with the material properties, specifically the Young's modulus, of the carbon fiber selected for this study, confirming the suitability of the chosen material for the optimization process. One of the most striking observations in the structural analyses was that the areas of maximum stress were located near the fixation points, which is contrary to the expected behaviour. Typically, the highest stresses are anticipated to occur further away from the fixed regions, but in this case, the maximum stresses were concentrated closer to the fixation areas. In Fig. 4, elastic strain exhibits different tendencies at angles A, B, and C, which contrasts with the observations in Fig. 3, where the equivalent stress distribution at different angles showed a different behavior. For instance, the area with maximum elastic strain in Fig. 4a is nearly twice as large as in Fig. 4b, while a completely different distribution is observed in Fig. 4c. A completely opposite behavior is observed in the total deformation map distribution compared to the elastic strain and equivalent stress values. While the maximum values for equivalent stress and elastic strain are found near the fixation area of the component, the total deformation exhibits its maximum values at the blade tips, gradually decreasing as it approaches the fixation area. All three angle images appear quite similar in the case of total deformation, much like the distribution maps of equivalent stress, where the three different angle views exhibit similar tendencies. Although the literature highlights that one of the primary challenges in developing turbine blades using the same material type (carbon fibers) is simultaneously reducing weight and enhancing load-bearing capacity [8,15–17], a similar approach is expected to be applicable to other components, such as the propeller in the current study. In this instance, an 11% weight reduction was achieved while ensuring that the structural integrity and safety of the component were preserved. This strategy seeks to optimize the balance between weight reduction and load bearing capability.

V. CONCLUSION

The topology optimization process successfully reduced the material use of the component while maintaining its structural integrity. The optimized design resulted in an 11.86% reduction in mass, demonstrating the efficacy of the optimization approach in enhancing material efficiency. Structural analysis revealed that most regions of the component experienced stress values below 20 GPa, with maximum stresses localized near the fixation points which is an unexpected outcome that deserves further investigation. The choice of carbon fiber reinforced thermoplastic composites was validated by their superior mechanical properties, which align with the literature values for Young's modulus. The findings confirm that carbon fiber reinforced composites are compatible for weight sensitive applications, such as propeller design, where both load bearing capacity and component's structural integrity are critical. Ultimately, the study highlights the potential of topology optimization in reducing component weight while preserving mechanical performance, offering valuable insights for future applications in aerospace, automotive, and other high performance industries.

REFERENCES

- [1] L. Lluri, B. Gërmënji, D. Hima, Carbon Fibers Offer Great Potential in the Automotive Industry, *Interdiscip. J. Res. Dev.* 6 (2019) 25. <https://doi.org/10.56345/ijrdv6n102>.
- [2] G.L. Song, C. Zhang, X. Chen, D. Zheng, Galvanic activity of carbon fiber reinforced polymers and electrochemical behavior of carbon fiber, *Corros. Commun.* 1 (2021) 26–39. <https://doi.org/10.1016/j.corcom.2021.05.003>.
- [3] A. Al-Mosawe, R. Al-Mahaidi, X.L. Zhao, Effect of CFRP properties, on the bond characteristics between steel and CFRP laminate under quasi-static loading, *Constr. Build. Mater.* 98 (2006) 489–501. <https://doi.org/10.1016/j.conbuildmat.2015.08.130>.
- [4] M. Pervaiz, S. Panthapulakkal, B. KC, M. Sain, J. Tjong, Emerging Trends in Automotive Lightweighting through Novel Composite Materials, *Mater. Sci. Appl.* 07 (2016) 26–38. <https://doi.org/10.4236/msa.2016.71004>.
- [5] Oak Ridge National Laboratory News, (2006). <https://www.ornl.gov/news/carbon-fiber-cars-could-put-us-highway-efficiency>.
- [6] B. Wang, J. Xiong, X. Wang, L. Ma, G.Q. Zhang, L.Z. Wu, J.C. Feng, Energy absorption efficiency of carbon fiber reinforced polymer laminates under high velocity impact, *Mater. Des.* 50 (2013) 140–148. <https://doi.org/10.1016/j.matdes.2013.01.046>.
- [7] J.S. Carlton, Propeller Materials, *Mar. Propellers Propuls.* 3 (2012) 385–396. <https://doi.org/10.1016/b978-0-08-097123-0.00018-6>.
- [8] B.A. Alshammari, M.S. Alsuhybani, A.M. Almushaikeh, B.M. Alotaibi, A.M. Alenad, N.B. Alqahtani, A.G. Alharbi, Comprehensive review of the properties and modifications of carbon fiber-reinforced thermoplastic composites, *Polymers (Basel)*. 13 (2021) 1–32. <https://doi.org/10.3390/polym13152474>.
- [9] C. Unterweger, J. Duchoslav, D. Stifter, C. Fürst, Characterization of carbon fiber surfaces and their impact on the mechanical properties of short carbon fiber reinforced polypropylene composites, *Compos. Sci. Technol.* 108 (2015) 41–47. <https://doi.org/10.1016/j.compscitech.2015.01.004>.
- [10] S. Hegde, B. Satish Shenoy, K.N. Chethan, Review on carbon fiber reinforced polymer (CFRP) and their mechanical performance, *Mater. Today Proc.* 19 (2019) 658–662. <https://doi.org/10.1016/j.matpr.2019.07.749>.
- [11] F. Li, Y. Liu, C.B. Qu, H.M. Xiao, Y. Hua, G.X. Sui, S.Y. Fu, Enhanced mechanical properties of short carbon fiber reinforced polyethersulfone composites by graphene oxide coating, *Polymer (Guildf)*. 59 (2015) 155–165. <https://doi.org/10.1016/j.polymer.2014.12.067>.
- [12] Y. Arao, S. Yumitori, H. Suzuki, T. Tanaka, K. Tanaka, T. Katayama, Mechanical properties of injection-molded carbon fiber/polypropylene composites hybridized with nanofillers, *Compos. Part A Appl. Sci. Manuf.* 55 (2013) 19–26. <https://doi.org/https://doi.org/10.1016/j.compositesa.2013.08.002>.
- [13] N.G. Karsli, A. Aytac, Tensile and thermomechanical properties of short carbon fiber reinforced polyamide 6 composites, *Compos. Part B Eng.* 51 (2013) 270–275. <https://doi.org/https://doi.org/10.1016/j.compositesb.2013.03.023>.
- [14] S.A. Mirdehghan, 1 - Fibrous polymeric composites, in: M.B.T.-E.P.F.M. Latifi (Ed.), *Text. Inst. B. Ser.*, Woodhead Publishing, 2021: pp. 1–58. <https://doi.org/https://doi.org/10.1016/B978-0-12-824381-7.00012-3>.
- [15] N. Forintos, T. Czigany, Multifunctional application of carbon fiber reinforced polymer composites: Electrical properties of the reinforcing carbon fibers – A short review, *Compos. Part B Eng.* 162 (2019) 331–343. <https://doi.org/https://doi.org/10.1016/j.compositesb.2018.10.098>.
- [16] X. Qin, Y. Lu, H. Xiao, Y. Wen, T. Yu, A comparison of the effect of graphitization on microstructures and properties of polyacrylonitrile and mesophase pitch-based carbon fibers, *Carbon N. Y.* 50 (2012) 4459–4469. <https://doi.org/10.1016/j.carbon.2012.05.024>.
- [17] D.K. Rajak, D.D. Pagar, P.L. Menezes, E. Linul, Fiber-reinforced polymer composites: Manufacturing, properties, and applications, *Polymers (Basel)*. 11 (2019). <https://doi.org/10.3390/polym11101667>.